Effect of the Pore Region of a Transmembrane Ion Channel on the Physical Properties of a Simple Membrane

Leonor Saiz,*,†,‡ Sanjoy Bandyopadhyay,§ and Michael L. Klein†

Chemistry Department and Center for Molecular Modeling, University of Pennsylvania, 231 South 34th Street, Philadelphia, Pennsylvania 19104-6323, NIST Center for Neutron Research, National Institute of Standards and Technology, 100 Bureau Drive, Stop 8562, Gaithersburg, Maryland 20899-8562, and Department of Chemistry, Indian Institute of Technology, Kharagpur 721 302, West Bengal, India

The effect of membrane proteins and peptides on their surrounding lipids is crucial for the structure, dynamics, and function of complex biological membranes as well as the interplay between membrane proteins and their environment. Here, we present a study of the influence of the transmembrane pore region of an ion channel on the physical properties of a phospholipid bilayer. We performed multinanosecond molecular dynamics simulations of the pore-forming aggregate of α-helical transmembrane peptides, which constitutes a model for the channel region of the nicotinic acetylcholine receptor, inserted in a simple lipid bilayer at conditions similar to those of the recent NMR experiments [Opella, S. J.; et al. *Nature Struct. Biol.* **1999**, *6*, 374]. The results obtained are compared with simulations of the pure lipid bilayer membrane. In particular, we consider here the simplest possible model membrane: a fully hydrated dimyristoyl-*sn*-glycerophosphocholine lipid bilayer, which is in the biologically relevant fluid lamellar phase at room temperature. Our analysis reveals that the peptides affect the properties of the lipid bilayer in several ways: (1) the bilayer thickness increases, (2) the number of gauche defects of the hydrocarbon chains decreases, (3) the orientational order of the hydrocarbon chains increases, (4) the orientational probability distribution of the lipid headgroup dipole moments becomes broader (more disordered), and (5) the lipid headgroup dipole moments are on average more oriented toward the water phase. Some of these effects depend on the specific properties of the case studied, such as the hydrophobic length of the bundle and the charges at the interface. Interestingly, the pore does not affect the two different sides of the membrane in the same way.

I. Introduction

Membrane proteins are key elements in many biological processes. Of particular interest are proteins or peptides that form pores in membranes, such as ion channels and antimicrobial peptides.[1,2] Recently, structural details about the function of important ion channels have emerged from experimental studies at atomic resolution.[3] In particular, it is currently known that one of the simplest possible motifs for the region of the protein linning the transmembrane channel pore consists of aggregates of amphiphilic α-helical segments. The study of peptide aggregation in membranes is thus becoming a fundamental problem. A detailed knowledge of the interactions present in these systems together with the general aspects of the thermodynamics will bring more insight into the mechanisms not only of folding of natural membrane proteins but also of action of antimicrobial peptides and other defense proteins.[4–6] The complexity of such systems for both experimental and theoretical approaches has stimulated the development of minimalistic synthetic models that retain most of the functional properties of the native system.[7–11]

Studies of proteins embedded in model membranes with different compositions demonstrated the interplay between protein (structure, dynamics, and function) and the properties of the supporting membrane.[12–14] Hydrophobic mismatch (difference between the hydrophobic length measured perpendicular

to the membrane surface of the membrane and the protein), membrane curvature, and in some systems, lipids promoting inverted hexagonal phases have been shown to be key elements that affect proteins. Furthermore, the incorporation of proteins or peptides into membranes is expected to modify the physical properties of model membranes, such as simple lipid bilayers.

The influence of single helical membrane peptides on the membrane properties has been studied experimentally. Non-associated membrane peptides within lipid bilayers have been shown to modify the phase behavior of the water–lipid system[15,16] and even promoted nonlamellar phases.[15] For instance, single transmembrane peptides can decrease the temperature of the phase transition and increase the orientational order of the lipid chains.[17] In contrast, a cationic peptide affected significantly only the membrane interface in another experiment.[18] Only recently were systematic studies performed using hydrophobic polypeptides of different lengths.[15] The results indicated that the hydrophobic mismatch induced by the peptides is minimized by the lipids. Differences obtained for peptides with different shapes indicate that the topography of the peptide surface has also a modulating effect.[15,17] In the case of associated transmembrane helical peptides, a stronger effect is expected because the diameter in the plane of the membrane of a peptide bundle is of the order of 20 Å-30 Å, quite large compared to that of the lipids (about 8 Å), whereas a single α-helical peptide is of the order of 10 Å. In these cases, the surface of the protein may act as a rigid wall and decrease the mobility of the lipids,[19] i.e., a reduction in entropy, as occurs, for instance, in liquids in confined geometries[20] and hydrophobic hydration in biomol-

† University of Pennsylvania.
‡ National Institute of Standards and Technology.
§ Indian Institute of Technology.

Pore Forming Peptides in a Simple Membrane

J. Phys. Chem. B, Vol. 108, No. 8, 2004 **2609**

ecules.[21] Indeed, very recent experiments on single helices suggest that the packing of lipids around peptides and around proteins is fundamentally different.[22] The authors observed that the membrane thickness of several model membranes was not modified by single hydrophobic peptides of different lengths,[22] whereas the order parameters of the hydrophobic chains slightly changed.[15]

Recent advances in computer technology have permitted the emergence of computer simulations and, especially, molecular dynamics (MD) as a powerful tool in biomembrane studies.[23] MD simulations can provide a detailed picture of the atomic and molecular motions and this microscopic information can be directly connected with the properties of experimental relevance. Computer simulation studies can thus be predictive and extremely useful in the interpretation of the experimental data. The level of detail available in atomistic MD simulations make this approach especially suited to study the effect of membrane embedded peptides on the properties of the lipid environment from an atomic perspective. With this aim, we performed multinanosecond MD simulations of the transmembrane pentameric bundle of the α-helical M2 segments embedded in a phospholipid bilayer model membrane. In particular, we consider here the simplest possible model membrane: a fully hydrated dimyristoyl-*sn*-glycerophosphocholine lipid bilayer, which is in the biologically relevant fluid lamellar phase at room temperature. This bundle constitutes the putative pore region of the nicotinic acetylcholine receptor (nAChR),[7,11,24] which is the neurotransmitter-gated ion channel responsible for the rapid propagation of electrical signals between cells at the nerve−muscle synapse.[1] It has been shown that the oligomerization of these M2 transmembrane helical domains of the nAChR in model membranes resulted in ion-channel activity with characteristics, such as conductance and selectivity, not identical but similar to those of the native protein.[7,11] Here, we focus on the influence of the embedded peptide bundle on the host membrane. Explicitly, we consider the two main effects investigated experimentally, namely, the effect on the lipid headgroups and on the order of the acyl chains. In contrast to earlier studies of similar pore-forming peptide aggregates as models for membrane proteins with ion-channel activity,[25,26] we paid special attention to investigate the type of lipid−peptide interactions occurring in the system, which may lead to the observed differences in the response of the lipid molecules to the presence of the peptide-bundle.

II. Methods

The model protein studied consisted of the transmembrane homopentameric bundle of the α-helical M2 segments of the nAChR glycoprotein. The peptide bundle was embedded in a fully hydrated 1,2-dimyristoyl-3-phosphatidylcholine (DMPC) lipid bilayer in the biologically relevant fluid lamellar phase, L_α. The M2 segments used in the present work correspond to the δ subunit of the native nAChR of the *Rattus norvegicus*. Each of the 25-residue peptides is characterized by the sequence GSEKMSTAISVLLAQAVFLLLTSQR, where residues G and R constitute the N- and C-terminal, respectively. The two termini are assigned to the intracellular (N) and extracellular or synaptic (C) side of the membrane.[11] The system with the previous characteristics contained 23 349 atoms and was constituted by 5 peptides, 94 DMPC lipid molecules (47 per monolayer, which corresponds to a lipid/peptide molar ratio of 19/1), 5 counterions, and 3434 water molecules. The initial coordinates for the α-helical M2 segments correspond to one of the 10 minimum energy configurations of the 1A11 PDB file.[11]
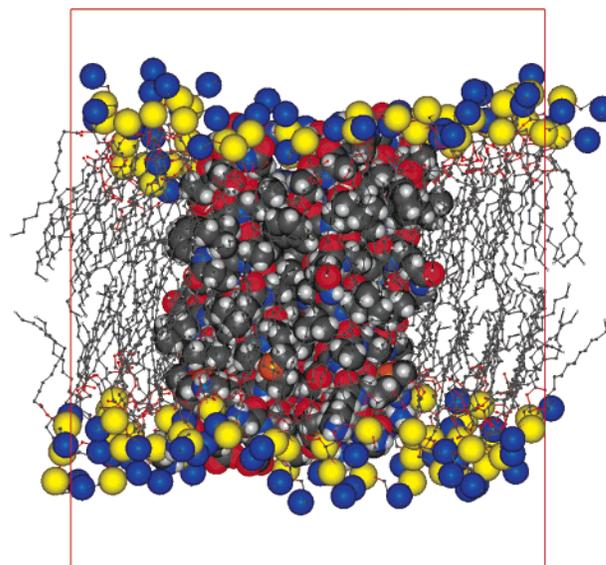

Figure 1. Configuration of the system taken from the MD simulation after 2.5 ns. The lipid molecules are shown as balls and sticks except for the N and P atoms of the headgroups, which are displayed as blue and yellow spheres, respectively. The water molecules and lipid hydrogen atoms are not shown for clarity. The coloring scheme for the M2 helices is N, blue; O, red; C, gray; H, white; and S, orange. The radii of the spheres correspond to the atomic van der Waals radii of the different species. The C-terminus (extracellular) is located at the top of the bundle.

Classical MD simulations were performed at constant temperature, $T = 303$ K, and pressure, $P = 1$ atm (1 atm = 101.3 kPa), (NPT ensemble) using periodic boundary conditions. Following the standard procedures, the simulations consisted of an equilibration period of about 2.5 ns during which the tilt of the α-helices evolved from the initial parallel orientation with respect to the membrane normal to their equilibrium value and an equilibrium run of 5 ns. The total simulation time is thus about 7.5 ns. Details of the initial setup and the equilibration of the system can be found elsewhere (Saiz and Klein, 2003; preprint). We used the Nosé−Hoover thermostat chain extended system isothermal−isobaric dynamics method, as implemented in the program PINY_MD,[27] with an orthorhombic simulation cell. We used a reversible multiple time step algorithm[28] with a time step of 4 fs, whereas the smallest time step was 1 fs. After equilibration, different properties were evaluated over the production run of 5 ns and were compared to those obtained during a 2 ns equilibrium run of a fully hydrated pure DMPC lipid bilayer in the L_α phase at similar conditions and with properties, such as, area per lipid, lamellar spacing, and orientational order parameters, in excellent agreement with experiment.[29] After the equilibrium was reached, the dimensions of the lipid bilayer evaluated over the additional 5 ns were $L_x = 55.2 \pm 0.6$ Å (1 Å = 10^{-10} m; all errors are given as stardard deviations), $L_y = 55.8 \pm 0.9$ Å, and $L_z = 71 \pm 1$ Å, where the $x−y$ plane corresponds to the plane of the interface and the z axis is parallel to the membrane normal. In Figure 1, we show a snapshot of the simulated system where only the polypeptides (highlighted at the center) and the lipid molecules within the simulation cell are shown.

The molecular and potential model used for the different components of the biomembranes was the recent version of the all-atom CHARMM force field[30−32] and the rigid TIP3P model for water.[33] During the simulations, all the motions involving hydrogen atoms were frozen using SHAKE/RATTLE algorithms. The short-range forces were computed using a cutoff
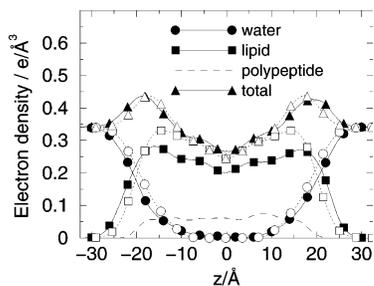
Figure 2. Electron density profiles: total and components arising from the water and lipid molecules for the mixed system (filled symbols and solid lines) and the pure lipid bilayer (opaque symbols and dotted lines) and from the peptides in the mixed membrane (dashed line). The bilayer center is located at $z = 0$ Å, and negative values of z correspond to the leaflet associated with the N-terminus.

of $\sim$10 Å and the minimum image convention, and the long-range forces were taken into account by means of the particle mesh Ewald (PME) technique.[34]

During the multinanosecond time scale investigated, the synthetic peptide bundle evolved from the initial configuration (where the amphipathic peptides were arranged as a pentamer, separated by about 12 Å with the hydrophilic residues facing the pore interior and the hydrophobic ones facing the lipids, and had their main axis oriented perpendicularly to the membrane surface) and adopted a left-handed coiled coil structure (Saiz & Klein, 2003; preprint). The calculated average tilt (angle) of the helices agrees well with the 12° obtained in recent NMR experiments at similar conditions.[11] The water-filled bundle displays a funnel-like architecture with the narrow region located at the C-terminus (synaptic), in agreement with the proposed model based on NMR experiments and energetic considerations.[11]

III. Results and Discussion

A. Density Profiles: Membrane Dimensions. To evaluate the hydrophobic mismatch between peptides and the lipid bilayer, it is important to know the atomic distributions of the different species in the direction perpendicular to the plane of the membrane surface (z) and compare the results with a pure lipid bilayer without the inserted peptide bundle. Computer simulation provides a clear way to express this, for instance, through the electron density profiles (EDPs), which can be computed for each atomic species and are proportional to the density profiles measured along the bilayer normal obtained by X-ray scattering experiments at low angles.[35] In Figure 2, we show the results obtained for the EDPs, and the different contributions separately, for the lipid bilayer with the peptide bundle (mixed system) and the pure DMPC lipid bilayer (pure system). The EDPs have been calculated by assuming a Gaussian distribution located at the atomic positions with variance, σ, equal to $\sigma = 2^{3/2}\sigma_{LJ}$, where σ_{LJ} is the range of the Lennard-Jones potential. The total EDP has features similar to those of pure lipid bilayer systems, i.e, a higher density at the position of the two lipid–water interfaces, specifically, of the headgroup region of the lipids and their hydration water, a lower density in the bulk water and hydrophobic region of membrane, and a slight depletion at the center of the membrane ($z = 0$ Å). Note that the distance between the two maxima in the total EDP (d_{pp}) is a measure of the bilayer thickness, whereas the region of overlapping densities of water and lipid molecules indicate the actual width of the interface.

The main effect of the incorporation of the peptide bundle into the DMPC lipid bilayer is a slight increase of the density

at the membrane center and an increase of the distance between the two maxima in the total EDP curve, indicating an increase in the bilayer thickness, compared to the pure membrane (from 35 to 38 Å). The former is due to the presence of the transmembrane peptides, which span the membrane interior. The close examination of the different components of the lipids at the interface, which give rise to the maxima in the EDPs, indicates that the latter is due to a shift of all the distributions (choline group, phosphate group, and carbonyl groups) toward further distances from the membrane center when compared to those of the pure lipid bilayer under similar conditions (data not shown). Therefore, the increase in bilayer thickness is basically a lengthening of the hydrophobic region of the bilayer (carbonyl groups separation increased from about 27 to 30 Å). These differences are amenable of experimental verification.

B. Lipid Orientational Order and Dynamics: Membrane Interior. The behavior of acyl chains in lipid bilayers is usually studied through the orientational order parameter, S_{CD}, which can be obtained experimentally by NMR spectroscopy and derived for each position, n, along the acyl chain. This orientational order parameter profile, $S_{CD}(n)$, can be calculated from the MD simulations and is given by $S_{CD}(n) = {}^1/_2\langle 3 \cos^2 \beta_n - 1 \rangle$, where β_n is the angle between the orientation of the vector along a C–H bond of the nth carbon atom of each chain and the bilayer normal. Here, the brackets indicate averages over time and lipid molecules. Thus, the $-S_{CD}(n)$ values for lipid bilayers are usually between 0 (random orientations) and 0.5 (perpendicular reference vectors).

In the mixed system, the presence of the bundle induces an increase of the orientational order of the DMPC lipid acyl chains compared to the pure lipid bilayer. This effect agrees qualitatively with the ordering observed experimentally for gramicidin in DMPC lipid bilayers,[15] even though the effect is more pronounced in the simulations. This enhanced effect might be in part due to the different (and larger) system and the fact that the temperature of the main phase transition for DMPC may be slightly different for the simulated lipid system and the natural (real) DMPC. The enhancement of ordering observed for the simulated mixed system is more significant for the C–H bonds located at positions deeper into the membrane interior. This effect is evidenced in Figure 3a, where we plot the $-S_{CD}$ for the DMPC lipid bilayer with and without the peptides and the results are compared with the experimental values for the pure system.[36] It is crucial to note that the membrane-spanning aggregate renders the two leaflets in the mixed system asymmetric, in contrast to the equivalent leaflets of pure lipid bilayer membranes. We obtained, however, similar results when the $-S_{CD}$ profiles were calculated separately for the two different monolayers (results not shown).

To further investigate this increase in orientational order, we calculated the profiles for the different lipids as a function of their distance from the bundle separately for both the extracellular and the intracellular leaflet. Three different regions were defined, which correspond to those lipids whose phosphate group lies within the range 0–16 Å (region A), 16–24 Å (region B), and 24–32 Å (region C) from the center of mass of the bundle. Even though, on average, the effect in both leaflets is similar, differences are evident when results for the different regions are compared. In the extracellular side of the membrane (results not shown), there is not a clear distinction of the behavior of lipids close to or far from the peptides and there is only a small difference for those lipids in close contact with the peptides, for which the order parameters for the carbon atoms at $n = 11$–13 are slightly higher than for the rest of the lipids.
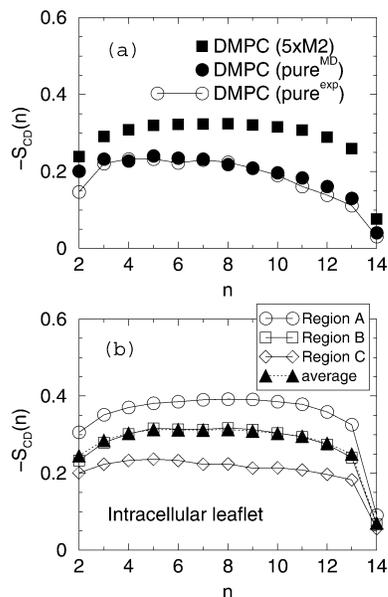
Pore Forming Peptides in a Simple Membrane

J. Phys. Chem. B, Vol. 108, No. 8, 2004 **2611**

Figure 3. (a) Orientational order parameter profiles for the mixed system and for the pure system from simulation and experiment.[36] (b) Results obtained for the intracellular leaflet as a function of the distance from the bundle (regions A, B, and C) and on average.
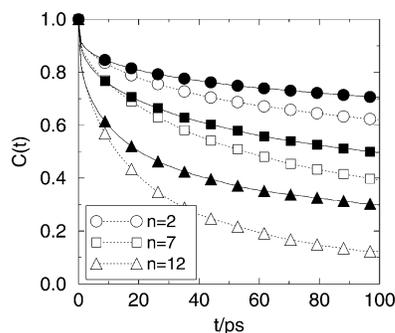

Figure 4. Reorientational time autocorrelation functions for the C_n-H vectors for $n = 2, 7,$ and 12 for the mixed (solid lines; full symbols) and the pure (dotted lines; opaque symbols) systems.

In contrast, at the intracellular side the effect on the order of the lipid acyl chains strongly depends on their distance from the bundle center (see Figure 3b). We found that in the region closest to the peptides, the orientational order further increases, which agrees well with previous simulations of gramicidin channels in DMPC lipid bilayers at different protein/lipid concentrations.[37,38] The order then decreases as the lipids are located farther from the bundle and the values are quite similar to those of the pure DMPC lipid bilayer in region C. Although the average behavior is almost identical, which indicates that the differences observed are not due to a different width of the peptide bundle at the two leaflets (a cylindrical shape is also evident in Figure 1), lipid molecules within the two different monolayers behave quite differently. Although one is quite homogeneous, the other one is extremely heterogeneous.

The increase of the orientational order parameters, which are related to both the conformation and the dynamics of the acyl chains, is correlated with, on one hand, a decrease of the number of gauche defects (data not shown) and, on the other hand, a fast short time reorientational dynamics of the chains whereas there is a slowing of the diffusive dynamics of the lipids. In Figure 4, we depict the reorientational correlation functions for the C−H vectors at different positions along the acyl chains for the mixed system and compare them with those of the pure
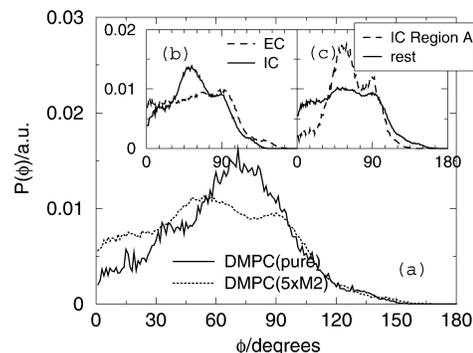

Figure 5. Probability distribution of the ϕ angle between the vector along the lipid headgroup dipole moment and the bilayer normal ($\phi = 90°$ corresponds to the membrane surface) in arbitrary units (a) for the average behavior for the pure lipid bilayer (solid line) and the mixed system (dotted line), (b) separately for lipids at the two different monolayers in the mixed system, and (c) for lipids in region A of the intracellular leaflet (dashed line) compared with the rest of lipids (solid line) in the mixed system.

system. Here, the reorientational molecular motions have been analyzed through the time correlation functions $C(t) = \langle \cos[\theta(t)] \rangle$, where $\theta(t)$ is the angle through which the considered molecule-fixed vector rotates in a time t. We calculated $C(t)$ for the vector along the C_n-H bond for $n = 2, ...,14$. The curves decay to a lower constant value for the pure lipid bilayer than for the mixed system, as expected from the lower values of the orientational order parameters. The fitting of the decay curves as a sum of (three) exponential terms plus a constant (within the time interval shown in Figure 4) indicates, however, that the correlation times associated with the $C(t)$ functions for the mixed system are lower than those for the pure lipid bilayer, except for those carbon atoms located close to the chain end. The (short time) reorientational dynamics for those lipid molecules in the mixed system is faster than for the pure lipid bilayer. Therefore, the peptide bundle can be envisaged as a *rigid nanotube* that restricts the mobility of the lipid molecules. This may be one of the main differences between isolated α-helices, which are similar in size to a lipid molecule, and transmembrane α-helical peptides when oligomerization takes place.

C. Lipid−Peptide Interactions and Headgroup Dipole Orientation: Membrane Interface. The α-helical peptides are mainly formed by neutral residues. Nevertheless, the presence of the two charged residues K (lysine; Lys$^+$) and E (glutamic acid; Glu$^-$) at the N-terminal (intracellular side) and the R (arginine; Arg$^+$) amino acid at the C-terminus (extracellular side), in addition to the charges associated with each (N- and C-) terminal extremity, would have an effect on the otherwise neutral biomembrane interface. On one hand, the change on the overall (net) charge of the interface will affect the average orientation of the lipid headgroup dipoles, a well-known effect from NMR studies.[39] In our system, the intracellular side of the membrane has a net positive charge. On the other hand, the possibility of specific lipid−peptide interactions, specifically Lys$^+$−headgroup interactions (note that these are the residues located at the more external part of the bundle), may lead to the formation of peptide-lipid complexes.

In Figure 5, we show the results obtained for the orientational probability distribution of the lipid headgroup dipole moments (basically, the P$^-$ → N$^+$ vectors connecting the phosphorus atom of the negative phosphate group and the nitrogen atom of the positive choline group) with respect to the bilayer normal, $P(\phi)$. The effect of embedding the peptide bundle consists of a broadening of the probability distribution of the headgroup

dipole orientations and an increase in the probability for orientations perpendicular to the interfacial plane, i.e., pointing toward the water phase, specially between 0° and 60° (Figure 5a). The clear maximum of the curve corresponding to the pure system, which indicates a prevalent orientation of the headgroup dipoles forming 70° with respect to the membrane normal, disappears and the mean value of the angle now is also shifted toward smaller angles (60°), in agreement with the results of NMR experiments on cationic peptides.[18] This is the expected trend because after incorporating the peptide bundle the intracellular side of the membrane has a net positive charge. Therefore, the positively charged choline groups tend to be expulsed from the membrane interface, where the lipid dipoles lay in the pure system, and the dipole moments are more likely to point toward the water region, decreasing in this way the average angle orientation with respect to the membrane normal.

The calculation of the orientational probability of the $P^- \rightarrow N^+$ vectors at the two interfaces indicates that both sides present rather different results (see Figure 5b), in contrast to what we observed for the orientational order parameters of the lipid chains. Although for the intracellular side the probability distribution function is qualitatively similar to that of the pure DMPC lipid bilayer, i.e., there is a preferential orientation of the headgroup dipoles but with the maximum shifted toward lower angles (from 70° to 60°), the lipids at the extracellular monolayer (EC) present an almost uniform distribution between 0 and 120°. This trend is similar to the effect of increasing temperature in pure lipid bilayers.[40] To investigate whether this behavior is affected by the position of the lipid with respect to the peptide bundle, we have calculated the $P(\phi)$ distributions for the lipids located within the regions A, B, and C, separately for the two different leaflets. In Figure 5c, the results show that the maximum in the $P(\phi)$ curve is mainly due to the lipids located in the region A of the intracellular side (IC). The rest of lipids display an almost uniform distribution. At the intracellular side, the behavior strongly depends on the position of the lipid. Close to the peptide, there is a preferential arrangement of the lipid headgroup dipoles forming 60° with the membrane normal. This seems to indicate the presence of lipids strongly interacting with the peripherical peptide amino acids.

To get some insight into whether this differential effect on the two membrane sides could be due to the formation of lipid–peptide complexes, we have studied the main peptide–lipid interactions. These interactions occur at the N-terminus (intracellular leaflet), where we observed that lipids behave differently as a function of the distance from the peptide-bundle. The most relevant are those interactions between the Lys$^+$ (external) residues and the lipid phosphate groups and the interactions of the N-cap residue, G, with the lipid phosphate groups. A detailed view of one of these lipid–peptide complexes is illustrated in Figure 6, where we show a Lys$^+$ residue forming a hydrogen bond with the phosphate group of a lipid molecule. From the computation of the radial distribution functions and the coordination numbers (data not shown), our results indicate that, on average, each peptide interacts with one lipid molecule through a Lys$^+$···P$^-$ (N–H···Op, where Op is the nonbonded oxygen atom of the lipid phosphate group) noncovalent bond and with about 0.6 molecules through a G···P$^-$ (N–H···Op) one. These two residues interact also with water molecules. In both cases, the most probable distance between the N atom of the K and G amino acids and the Op atoms of the lipids is about 2.8 Å. Because these are strong and long-lived (with respect to the time scale of the simulations) interactions, it is reasonable to expect a different behavior for the leaflet (intra-
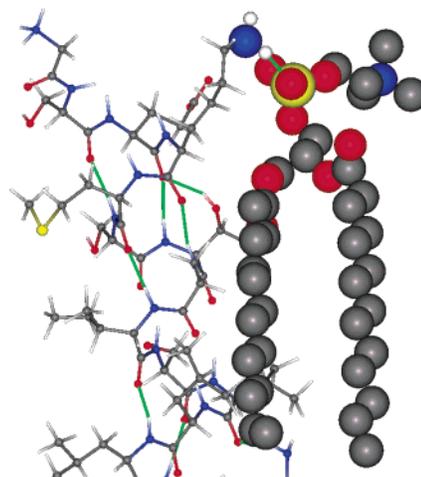

Figure 6. Detail of a lipid–peptide complex extracted from an instantaneous configuration of the simulated system. The Lys$^+$ residue of one of the peptides interacts with the phosphate group of a DMPC lipid molecule. The peptide is displayed in a ball-and-stick fashion, and the lipid molecule and the NH$_3$ group of the Lys$^+$ residue are represented by spheres with the covalent radii of the different species. For simplicity, only the hydrogen atoms of the peptides are shown. The color code is that of Figure 1. Hydrogen bonds are shown in green.

cellular) where these interactions are present. As discussed in the previous section, the most inhomogeneous effect of the peptide bundle on the studied properties of both the headgroups and the chains of the lipids is found in the intracellular monolayer. There, the behavior depends on the distance from the lipid to the bundle. Conversely, lipid molecules at the extracellular side are affected in an homogeneous fashion.

IV. Conclusions

Knowledge of the effect of membrane peptides on the lipid environment is crucial for the understanding of the structure, dynamics, and function of complex biological membranes and the interplay between membrane proteins and their environment. Early experiments aimed to study the modification of the properties of the lipid environment by the addition of membrane peptides or proteins obtained diverse results that were difficult to connect between them.[15−19,22] The main reason was the different conditions of the experiments, the lack of systematic studies, and the complexity of the systems. Recent molecular dynamics simulations have proved their ability to study transmembrane proteins in their natural environment with full atomic detail.[41,42]

Here, we have investigated the effect of the presence of a model transmembrane pore region of an ion-channel protein on the properties of the host membrane by means of atomistic computer simulations. Specifically, we have performed an MD simulation study of a pore-forming pentameric bundle of α-helical polypeptides embedded in a (DMPC) lipid bilayer and the results have been compared with those of a pure lipid bilayer membrane with properties in excellent agreement with experiment. This peptide aggregate constitutes a model for the channel of the nicotinic acetylcholine receptor, the ligand-gated ion channel responsible for the fast propagation of electrical signals between cells.

We focused on the main properties studied experimentally, namely, the effect on the membrane interior and on the lipid–water interface. We found that the main effects are an increase of the bilayer thickness, a decrease of the number of gauche defects of the lipid acyl chains, an increase of the orientational order parameters of the hydrocarbon chains, and a more

Pore Forming Peptides in a Simple Membrane

J. Phys. Chem. B, Vol. 108, No. 8, 2004 **2613**

disordered disposition of the lipid headgroup dipole moments at the membrane interface, which are on average more oriented toward the water phase. Some of these effects depend on the specific properties of the case studied, such as the hydrophobic length of the bundle and the net charge of the interface. The degree of detail available in the simulations permitted the calculation of the average properties, which are amenable to experimental verification, as well as the different properties for the lipid molecules in the two different monolayers and as a function of their distance from the peptides. Interestingly, we observed a different behavior for the lipid molecules at the two monolayers (C- and N-terminus sides). Strong and long-lived (electrostatic) lipid−peptide interactions are present only in the intracellular monolayer (N-terminus) where the lipid molecules present a heterogeneous behavior; i.e., the degree of response of the molecules depends on how far they are from the peptides. In contrast, at the other side, the molecules respond in a more uniform way, as a whole, to the presence of the peptide bundle.

In summary, the molecular dynamics approach used in this work has shown that membrane peptides affect not only the general physical properties of the host membrane but also the local behavior of the lipid molecules. Furthermore, the identification of specific lipid−peptide interactions may be crucial for future studies aimed at correlating these complexes with the differences observed in the local behavior of the lipid molecules.

References and Notes

(1) Hille, B. *Ionic Channels of Excitable Membranes*; Sinauer Associates Inc.: Sunderland, 1992.

(2) Zasloff, M. *Nature* **2002**, *415*, 389.

(3) Doyle, D. A.; Cabral, J. M.; Pfuetzner, R. A.; Kuo, A. L.; Gulbis, J. M.; Cohen, S. L.; Chait, B. R.; MacKinnon, R. *Science* **1998**, *280*, 69.

(4) Popot, J. L.; Engelman, D. M. *Biochemistry* **1990**, *29*, 4031.

(5) Huang, H. W. *Biochemistry* **2000**, *39*, 8347.

(6) White, S. H.; Wimley, W. C. *Annu. Rev. Biophys. Biomol. Struct.* **1999**, *28*, 319.

(7) Oiki, S.; Danho, W.; Madison, V.; Montal, M. *Proc. Natl. Acad. Sci. U.S.A.* **1988**, *85*, 8703.

(8) Lear, J. D.; Wasserman, Z. R.; DeGrado, W. F. *Science* **1988**, *240*, 1177.

(9) Duff, K. C.; Ashley, R. H. *Virology* **1992**, *190*, 485.

(10) Tew, G. N.; Liu, D.; Chen, B.; Doerksen, R. J.; Kaplan, J.; Caroll, P. J.; Klein, M. L.; DeGrado, W. F. *Proc. Natl. Acad. Sci. U.S.A.* **2002**, *99*, 5110.

(11) Opella, S. J.; Marassi, F. M.; Gesell, J. J.; Valente, A. P.; Kim, Y.; Oblatt-Montal, M.; Montal, M. *Nature Struct. Biol.* **1999**, *6*, 374.

(12) Bloom, M. *Biol. Skr. Dan. Vid. Selsk.* **1998**, *49*, 13.

(13) Brown, M. F. *Chem. Phys. Lipids* **1994**, *73*, 159.

(14) Andersen, O. S.; Nielsen, C.; Maer, A. M.; Lundæ, J. A.; Goulian, M.; Koeppe, R. E. *Biol. Skr. Dan. Vid. Selsk.* **1998**, *49*, 75.

(15) de Planque, M. R. R.; Greathouse, D. V.; Koeppe, R. E., II; Schäfer, H.; Marsh, D.; Killian, J. A. *Biochemistry* **1998**, *37*, 9333.

(16) Zein, M.; Winter, R. *Phys. Chem. Chem. Phys.* **2000**, *2*, 4545.

(17) Paré, C.; Lafleur, M.; Liu, F.; Lewis, R. N. A. H.; McElhaney, R. N. *Biochim. Biophys. Acta* **2001**, *1511*, 60.

(18) Roux, M.; Neumann, J. M.; Hodges, R. S.; Devaux, P. F.; Bloom, M. *Biochemistry* **1989**, *28*, 2313.

(19) Barrantes, F. J. *Mol. Membr. Biol.* **2002**, *19*, 277.

(20) Liu, G.; Li, Y.; Jonas, J. *J. Chem. Phys.* **1991**, *9*, 68921.

(21) Cheng, Y. K.; Rossky, P. J. *Nature* **1998**, *392*, 696.

(22) Weiss, T. M.; van der Wel, P. C. A.; Killian, J. A.; Koeppe, R. E., II; Huang, H. W. *Biophys. J.* **2003**, *84*, 379.

(23) See for instance: Saiz, L.; Klein, M. L. *Acc. Chem. Res.* **2002**, *35*, 482. Pastor, R. W.; Venable, R. M.; Feller, S. E. *Acc. Chem. Res.* **2002**, *35*, 438. Roux, B. *Acc. Chem. Res.* **2002**, *35*, 366.

(24) Miyazawa, A.; Fujiyoshi, Y.; Unwin, N. *Nature* **2003**, *423*, 949.

(25) Tieleman, D. P.; Forrest, L. R.; Sansom, M. S. P.; Berendsen, H. J. C. *Biochemistry* **1998**, *37*, 17554.

(26) Husslein, T.; Moore, P. B.; Zhong, Q. F.; Newns, D. M.; Pattnaik, P. C.; Klein, M. L. *Faraday Discuss.* **1998**, *111*, 201.

(27) Tuckerman, M. E.; Yarne, D. A.; Samuelson, S. O.; Hughes, A. L.; Martyna, G. J. *Comput. Phys. Commun.* **2000**, *128*, 333.

(28) Tuckerman, M. E.; Berne, B. J.; Martyna, G. J. *J. Chem. Phys.* **1992**, *97*, 1990.

(29) Bandyopadhyay, S.; Shelley, J.; Klein, M. L. *J. Phys. Chem. B* **2001**, *105*, 5979.

(30) Schlenkrich, M.; Brickmann, J.; MacKerell, A. D., Jr.; Karplus, M. In *Biological membranes: A molecular perspective from computation and experiment*; Merz, K. M., Jr., Roux, B., Eds.; Birkhauser: Boston, 1996; p 31.

(31) Feller, S. E.; MacKerell, A. D., Jr. *J. Phys. Chem. B* **2000**, *104*, 7510.

(32) MacKerell, A. D., Jr.; et al. *J. Phys. Chem. B* **1998**, *102*, 3586.

(33) Jorgensen, W. L.; Chandrasekhar, J.; Madura, J. D.; Impey, R. W.; Klein, M. L. *J. Chem. Phys.* **1983**, *79*, 926.

(34) Darden, T.; York, D.; Pedersen, L. *J. Chem. Phys.* **1993**, *98*, 10089.

(35) White, S. H.; Wiener, M. C. *Biophys. J.* **1992**, *61*, 434.

(36) Douliez, J. P.; Leonard, A.; Dufourc, E. J. *Biophys. J.* **1995**, *68*, 1727.

(37) Woolf, T. B.; Roux, B. *Proteins: Struct., Funct. Genet.* **1996**, *24*, 92.

(38) Chiu, S.-W.; Subramaniam, S.; Jakobsson, E. *Biophys. J.* **1999**, *76*, 1929.

(39) Seelig, J.; Macdonald, P. M.; Scherer, P. G. *Biochemistry* **1987**, *26*, 7535.

(40) Saiz, L.; Klein, M. L. *J. Chem. Phys.* **2002**, *116*, 3052.

(41) Berneche, S.; Roux, B. *Nature* **2001**, *414*, 73.

(42) Tajkhorshid, E.; Nollert, P.; Jensen, M. O.; Miercke, L. J. W.; O'Connell, J.; Stroud, R. M.; Sculten, K. *Science* **2002**, *296*, 525.